Available online at www.sciencedirect.com
SCIENCE DIRECT
Journal of Solid State Chemistry 179 (2006) 2739–2743
JOURNAL OF SOLID STATE CHEMISTRY
www.elsevier.com/locate/jssc

Rapid communication

Pressure-induced polymorphism in Al_3BC_3: A first-principles study

Jingyang Wang[a,b,*], Yanchun Zhou[a], Zhijun Lin[a,c], Ting Liao[a,c]

[a]*Shenyang National Laboratory for Materials Science, Institute of Metal Research, Chinese Academy of Sciences, 72 Wenhua Road, Shenyang, 110016, PR China*

[b]*International Centre for Materials Physics, Institute of Metal Research, Chinese Academy of Sciences, Shenyang 110016, PR China*

[c]*Graduate School of Chinese Academy of Sciences, Beijing 100039, PR China*

Received 16 February 2006; received in revised form 25 April 2006; accepted 21 May 2006
Available online 25 May 2006

Abstract

Al_3BC_3, an isostructural phase to Mg_3BN_3, experienced no pressure-induced phase transformation that occurred in the latter material (J. Solid State Chem. 154 (2000) 254–256). The discrepancy is not clear yet. Using the first-principles density functional calculations, we predict that Al_3BC_3 undergoes a hexagonal-to-tetragonal structural transformation at 24 GPa. The predicted phase equilibrium pressure is much higher than the previously reported pressure range, i.e., 2.5–5.3 GPa, conducted on phase stability of Al_3BC_3. A homogeneous orthorhombic shear strain transformation path is proposed for the phase transformation. The transformation enthalpy barrier is estimated to yield a low value, i.e., 0.129 eV/atom, which ensures that the transformation can readily take place at the predicted pressure.

Keywords: Al_3BC_3; High pressure; Phase transformation; Density functional calculations; Equation of state

1. Introduction

Al_3BC_3 was recently investigated as a promising ceramic of high hardness and toughness, as well as of high chemical and thermal stability, in lightweight structures [1]. Hillebrecht and Meyer [2] successfully synthesized and solved the crystal structure of Al_3BC_3 a few years ago. This phase was determined to crystallize with space group $P6_3/mmc$, and its crystal structure was described as follows: isolated C atoms are located at the center of corner-sharing Al_5 trigonal bipyramids which are interleaved by short linear C–B–C units along the *c*-axis.

The C–B–C unit in Al_3BC_3 was characterized with a nature of strong covalent bonding by experimental vibrational spectroscopy [2]. Furthermore, electronic structure and bonding characteristics were reported for Al_3BC_3 using density functional calculations [3]. However, this compound is much less known about its mechanical properties. The reason is attributed to difficulties in synthesizing bulk and/or single crystalline material. Equation of state of Al_3BC_3 has been experimentally studied by Solozhenko et al. [4]. Bulk modulus and weak anisotropic compressibility were reported as 153 GPa and $k_c/k_a = 1.06$, respectively. The authors have conducted theoretical studies of the elastic stiffness of Al_3BC_3 recently [5]. Although Al_3BC_3 has a bulk modulus of 158 GPa, the material experiences unusual low shear modulus c_{44} of only 16 GPa. The underlying origin of low shear-strain resistance was proposed with two simultaneously occurred processes: the rigid linear C–B–C units tilt with respect to the *c*-axis easily, and simultaneously, the corner-sharing Al_5C bypyramid slabs shear slide along the basal plane with low resistance. As is known that $c_{44} > 0$ represents a measure of the stability condition for hexagonal crystal, and low magnitude of c_{44} may be important for better understanding the phase stability, such as polymorphism arisen from shear-strain induced instability.

Comprehensive understanding of phase stability of Al_3BC_3 is desirable for its development as a promising structural material. Mg_3BN_3, an isostructural phase to Al_3BC_3, was found to crystallize in different structures

*Corresponding author. Shenyang National Laboratory for Materials Science, Institute of Metal Research, Chinese Academy of Sciences, 72 Wenhua Road, Shenyang, 110016, PR China. Fax: +86 24 23891320.
E-mail address: jywang@imr.ac.cn (J. Wang).

0022-4596/$ - see front matter © 2006 Elsevier Inc. All rights reserved.
doi:10.1016/j.jssc.2006.05.016

depending on the pressure applied [6,7]. The low-pressure polymorph has a hexagonal cell (space group $P6_3/mmc$, $Z = 2$) [6], and the high-pressure form is determined with a orthorhombic cell (space group $Pmmm$, $Z = 1$) [7]. Hiraguchi et al. [7] reported a hexagonal-to-orthorhombic phase transformation at 4 GPa and 1500 K. Similar phase transformation was also expected for Al_3BC_3. Unfortunately, Al_3BC_3 was reported to undergo no structural transformation up to 1800 K over the 2.5–5.3 GPa pressure range [4]. The reason was not well established yet.

The present work was aimed at studying high-pressure structural stability of Al_3BC_3 using first-principles computations. We predicted a hexagonal-to-tetragonal structural transformation for Al_3BC_3 at a pressure about 24 GPa, and proposed a homogeneous orthorhombic shear strain transformation path with very low transformation enthalpy barrier. For comparison, the phase transformation pressure was calculated about 2 GPa for Mg_3BN_3, which was in good agreement with previous experimental result.

2. Computational details

The CASTEP code was used in the present calculations [8], wherein the Vanderbilt-type ultrasoft pseudopotential [9] and local density approximation were employed. The plane-wave basis set cut-off was 450 eV for all calculations. The special points sampling integration over the Brillouin zone was employed by using the Monkhorst–Pack method with a $10 \times 10 \times 2$ special k-points mesh [10].

To investigate the ground state electronic structure and equation of state, the equilibrium crystal structures were optimized at various isotropic hydrostatic pressures ranging from 0 to 50 GPa. Lattice parameters, including lattice constants and internal atomic positions, were modified independently to minimize the enthalpy and interatomic forces. The anisotropic responses of studied compounds to applied hydrostatic pressure were considered by optimizing the lattice parameters a and c independently until three diagonal components of stress tensor were all equal to the applied pressure. We have calculated the ratio between linear compressibility coefficients in the c direction and along the basal plane. The obtained theoretical ratio of 1.05 was in excellent agreement with the experimental value of 1.06 [4]. The Broyden–Fletcher–Goldfarb–Shanno (BFGS) minimization scheme [11] was used in geometry optimization. The convergent tolerances for geometry optimization were: difference on total energy within 5×10^{-6} eV/atom, maximum ionic Hellmann–Feynman force within 0.01 eV/Å, maximum ionic displacement within 5×10^{-4} Å and maximum stress within 0.02 GPa. The authors have shown that the present first-principles calculation scheme is reliable on predicting crystal structure, elastic stiffness and inter-atomic force constants of ternary carbides [12–14] and complex oxides, like $LaPO_4$ and $CaWO_4$ [15].

3. Results and discussions

3.1. Pressure-induced phase transformation

In Fig. 1, we present the bond-length contractions of hexagonal Al_3BC_3 under various pressures, together with the relative unit cell volume, V/V_0, as a function of external pressure plotted in the inset. The strengths of interatomic bonds were estimated by their resistances against external pressures. The highest lying curve is associated with the B–C bond, which shows its most resistive character against hydrostatic pressure. This is coincident with the strongest covalent binding within the linear C–B–C unit [2]. Lower located curves are of Al–C bond coupling the Al_5C slab and C–B–C unit, and Al–C bond residing along the basal plane. The two curves are hard to be distinguished, which suggests similar bonding strengths against compression. The lowest lying curve corresponds to the Al–C bond residing along the c direction and displays the most compressible feature. In addition, by fitting the data plotted in the inset of Fig. 1 with the Birch–Murnaghan equation [16], bulk modulus B_0 was obtained as 158 GPa, which was in good agreement with the experimental value, 153 GPa [2].

To calculate the theoretical structural parameters of high-pressure phases, geometry optimizations were performed using the experimental Mg_3BN_3-type structure with orthorhombic symmetry [7]. It should be stated that the optimized crystal structure converged to a tetragonal structure (space group $P4/mmm$) for the possible high-pressure phase. The present theoretical structure yields higher symmetry compared to the previously reported orthorhombic structure (space group $Pmmm$) with unequal a and b parameters [7]. Table 1 summarizes the optimized structural parameters of hexagonal (h-phase) and tetragonal (t-phase) polymorphs of Al_3BC_3 and Mg_3BN_3. Previous experimental results are included for comparison [2,6,7]. Satisfactory agreement is achieved between the

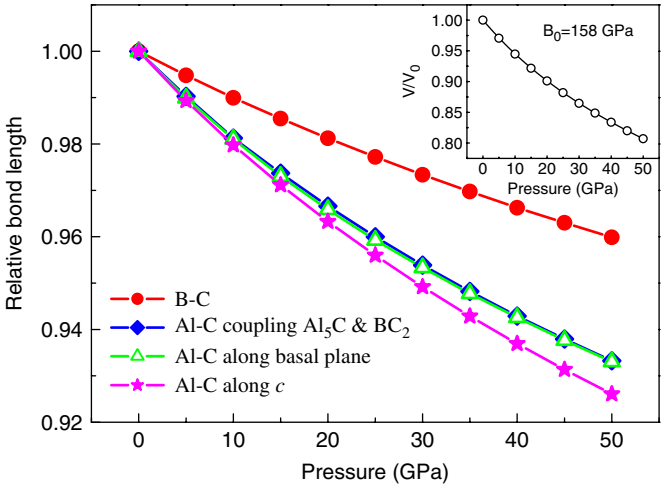

Fig. 1. Bond-length contractions in Al_3BC_3 under various pressures, together with the equation of state shown in the inset.

Table 1
Computed crystal structures of *h*-(hexagonal) and *t*-(tetragonal) Al_3BC_3 and Mg_3BN_3 phases, together with experimental data for comparison

Compound	Method	Space group	*a* (Å)	*c* (Å)	Internal coordinates
h-Al_3BC_3	Calc.	$P6_3/mmc$	3.363	15.58	$z_C = 0.0914$ $z_{Al} = 0.1224$
	Expt. [2]	$P6_3/mmc$	3.401	15.84	
t-Al_3BC_3	Calc.	$P4/mmm$	2.971	7.403	$z_C = 0.3073$ $z_{Al} = 0.2619$
h-Mg_3BN_3	Calc.	$P6_3/mmc$	3.513	15.99	$z_N = 0.0836$ $z_{Mg} = 0.1229$
	Expt. [6]	$P6_3/mmc$	3.544	16.04	$z_N = 0.0851$ $z_{Mg} = 0.1228$
t-Mg_3BN_3	Calc.	$P4/mmm$	3.066	7.829	$z_N = 0.3290$ $z_{Mg} = 0.2569$
	Expt. [7]	$Pmmm$	3.093 (3.134)	7.701	$z_N = 0.3262$ $z_{Mg} = 0.2670$

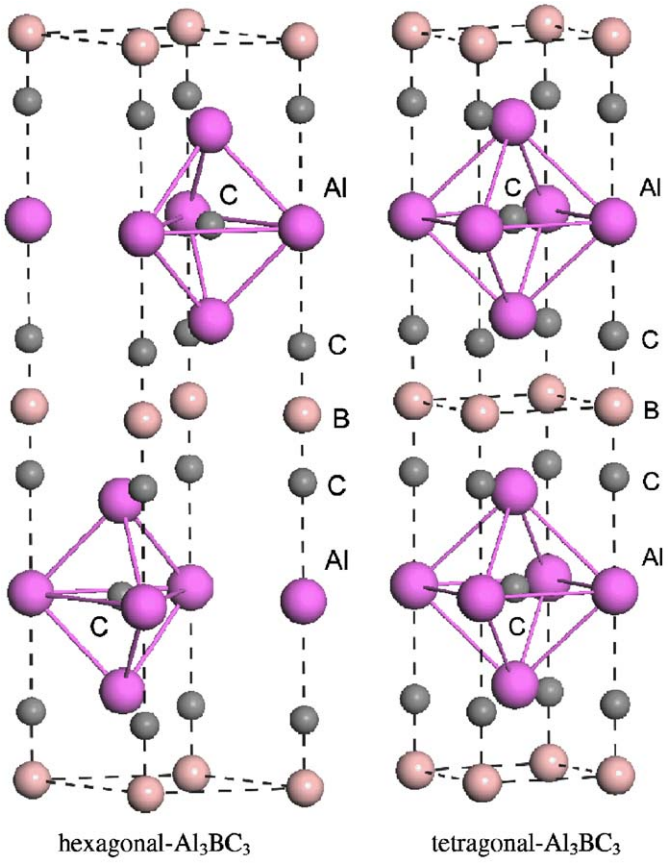

Fig. 2. Crystal structures of hexagonal- and tetragonal-Al_3BC_3. Two unit cells are plotted for tetragonal structure along the *c* direction for making comparisons conveniently. The highlighted Al–C units show predominant structural differences on bonding coordination between Al and C atoms.

present calculations and previous works. As shown in Table 1, all theoretical lattice constants deviate from experimental values within 1.7%. Furthermore, the computed internal degrees of freedom z_{Atom} also coincide well with experimental results. The crystal structure of low-pressure hexagonal Al_3BC_3 is compared with that of high-pressure tetragonal phase in Fig. 2. The Al (4*f* Wyckoff position) and C (2*d* Wyckoff position) atoms in the hexagonal Al_3BC_3 structure change to the more symmetrical central positions in the tetragonal Al_3BC_3 structure, leading to a different bonding coordination between Al and C atoms along the basal plane. Furthermore, the symmetry of the resultant tetragonal structure halves the *c*-axis.

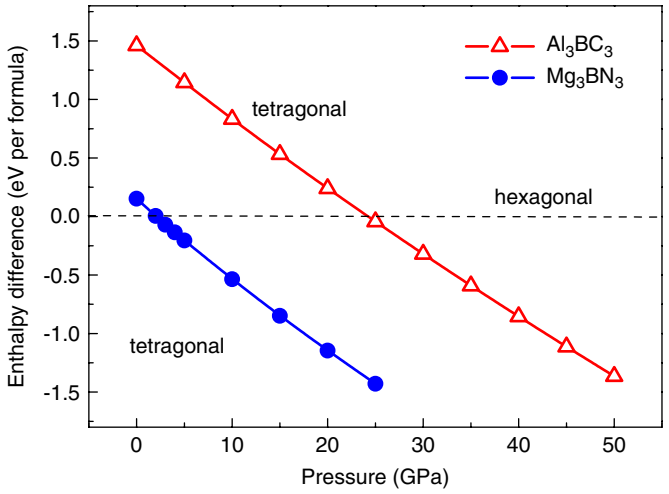

Fig. 3. Relative enthalpy of tetragonal phase with respect to hexagonal phase at various pressures. The crossing occurs at about 2 and 24 GPa for Mg_3BN_3 and Al_3BC_3, respectively.

To investigate the pressure-induced structural transformation, we optimized both the cell parameters and internal degrees of freedom for hexagonal and tetragonal phases under each external hydrostatic pressure. Fig. 3 shows the enthalpy differences from hexagonal phase for Al_3BC_3 and Mg_3BN_3 up to 50 GPa. At the ambient pressure, the enthalpy differences are 0.15 and 1.46 eV/formula for Mg_3BN_3 and Al_3BC_3, respectively. Upon applying pressure, hexagonal phase remains a low energy structure until the enthalpy of the tetragonal phase becomes lower than that of hexagonal phase. Such a crossing indicates a thermodynamic instability of the hexagonal phase and a possible structural transition to the tetragonal phase. The

enthalpy of tetragonal phase crosses that of hexagonal phase at pressures about 2 and 24 GPa for Mg_3BN_3 and Al_3BC_3, respectively.

Previous experimental study reported a phase transition occurred for Mg_3BN_3 at a pressure about 4 GPa [7], which agrees well with the present calculation. For Al_3BC_3, we predicted a much higher phase-transformation pressure than that of Mg_3BN_3. Also, the predicted phase-transformation pressure is far beyond the previously conducted pressure range on phase stability of Al_3BC_3 [2]. It should be noted that the enthalpy differences vary with pressures in the same tendency for Mg_3BN_3 and Al_3BC_3 as shown in Fig. 3, therefore, the high phase-transformation pressure of Al_3BC_3 is due to the large energy difference between the polymorphs at ambient conditions.

3.2. Transformation path and enthalpy barrier

The phase equilibrium transformation pressures have been calculated for Al_3BC_3 and Mg_3BN_3 in the previous section. However, there may be large kinetic barriers that impede the transition at the equilibrium pressure, leading to a hysteresis between the forward and backward transformations. This means, in order for the actual transformation process to take place, not only the enthalpy of the ending phase (in this case tetragonal phase) should be lower than or equal to the starting phase (in this case hexagonal phase), but also the enthalpy barrier of the transformation between the two phases has to be sufficiently low. Since the barrier of transformation has an influence on the transformation pressure, it is necessary to study the barrier for selected transformation path to better understand the possibility of phase transformation.

Hiraguchi et al. [7] have compared the crystal structure of hexagonal and orthorhombic Mg_3BN_3, and proposed an evident correlation of the two structures. They speculated that, at high pressure/high temperature, the Mg (4*f* Wyckoff position) and N (2*d* Wyckoff position) atoms in the hexagonal structure shift to the more symmetrical central positions along the basal plane, with a concomitant change of the hexagonal cell into an orthorhombic cell, to produce the orthorhombic structure. Very recently, Limpijumnong et al. [17,18] described a homogeneous in-plane orthorhombic strain transformation path from the hexagonal to the cubic structure for GaN and ZnO, and analyzed its energetics using first-principles total energy calculations. Previous works have proposed a possible transformation path linking the two studied polymorphs by undergoing in-plane shear deformation.

In order to understand the proposed phase transformation path, the relationship between crystal structures of two end phases are reinvestigated at first. The hexagonal crystal structure is characterized by three parameters, the lattice constants a, c, and the internal parameter z which fixes the relative position of the hexagonal close-packed sublattices along the c direction. The last parameter has to be relaxed when a uniaxial strain is applied in the c direction. With respect to the hexagonal-to-tetragonal phase transformation, the c changes from $c_h = 15.58$ Å to $c_t = 14.81$ Å (2 times the c constant of tetragonal structure), leading a c_h/c_t ratio decreases from 1.052 to 1. The projected hexagonal and tetragonal structures on the (001) plane are shown in Fig. 4. As seen from the top view figures, the hexagonal crystal is equivalent to the side-centered orthorhombic structure with the structure parameters a and b of $b/a = 1.733$. To characterize the hexagonal-symmetry-breaking in-plane strain, two parameters, the b/a ratio and the internal parameter v, are introduced following Refs. [16,17]. The additional internal parameter v defines the relative in-plane projection of two sublattices, and yields $v = 0.333$ and 0.5 for hexagonal and tetragonal structures, respectively. Thereafter, the hexagonal-to-tetragonal phase transformation can be described by an additional in-plane orthorhombic shear strain b/a, which would vary from 1.733 to 1 gradually. In the present calculation, both z and v were optimized for each strained structure.

To study the possible paths of hexagonal-to-tetragonal phase transformation, one should map out the enthalpy surface as a function of two independent strain parameters, c_h/c_t and b/a varied from 1.502 to 1 and 1.733 to 1, respectively, at the calculated equilibrium transformation pressure. The most favorable path is that yielding the

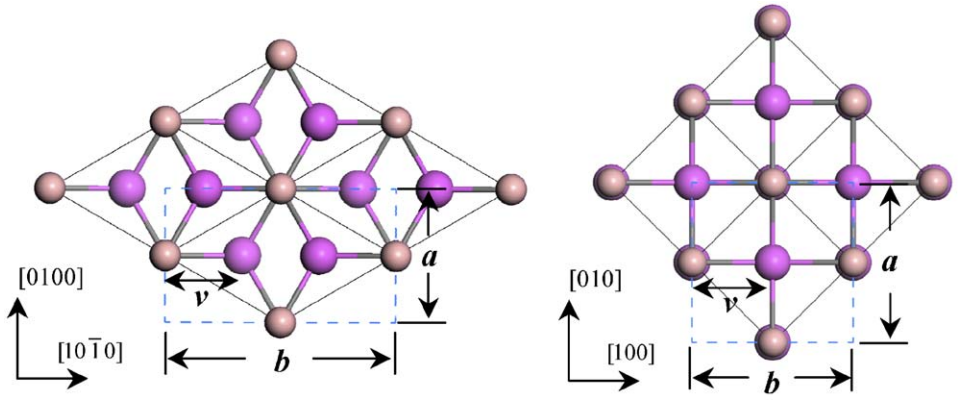

Fig. 4. Top views of hexagonal and tetragonal crystal structures. The parameters b, a, and v defining the structure are illustrated (i.e., $b/a = 1.733$ and $v = 0.333$, and $b/a = 1.0$ and $v = 0.5$ for hexagonal and tetragonal structures, respectively).

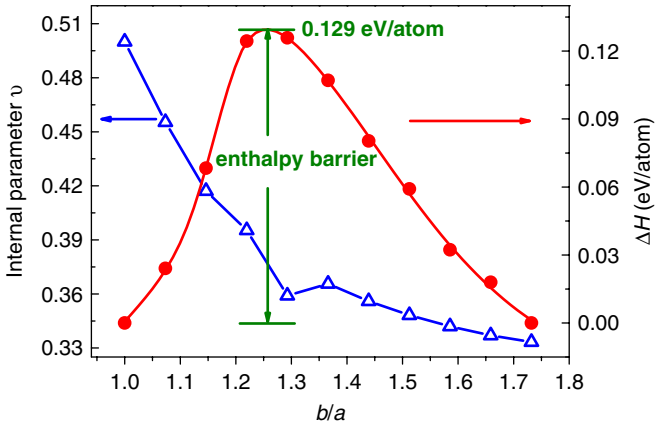

Fig. 5. Enthalpy difference at the equilibrium transformation pressure $P = 24$ GPa for Al_3BC_3 along the proposed transformation path. Internal structural parameter v as a function of b/a strain is also included. The low enthalpy barrier, 0.129 eV/atom, ensures phase transformation being readily occurred at this predicted pressure.

smallest enthalpy barrier. However, it is very computational consuming to map out the whole enthalpy surface. Pressure-induced hexagonal-to-cubic phase transformations in ZnO and GaN have been proposed along the straight diagonal transformation path [17,18], and therefore, we only adopted the same transformation path in the c_h/c_t–b/a space. The change in enthalpy along the chosen transformation path at the equilibrium transition pressure $P = 24$ GPa is shown in Fig. 5. The obtained transformation barrier yields a notably low value, i.e., 0.129 eV/atom. This transformation barrier is very close to the critical enthalpy barrier, e.g., 0.125 eV/atom of the hexagonal-to-cubic phase transformation in ZnO, AlN, GaN, and SiC [18]. Therefore, the transformation can readily take place at the phase equilibrium pressure $P = 24$ GPa.

Fig. 5 also includes the trend of internal structural parameter v as a function of in-plane strain b/a. An abrupt change takes place near the critical strain with the maximum enthalpy barrier. Before the in-plane strain b/a reaches its critical value, the two sublattices are basically locked at their initial positions, which suggests that the directional sp^2 type Al-C covalent bond is highly stable and favors the 3-fold coordination along the basal plane. Beyond the critical value, the two sublattices slide along the basal plane to the symmetrical central position, leading to the internal structural parameter v converging rapidly up to 0.5. Thereafter, Al and C atoms experience 4-fold coordination along the basal plane in the tetragonal phase.

4. Conclusions

Using the first-principles density functional calculations, we studied the phase stability of Al_3BC_3 and Mg_3BN_3 under isotropic hydrostatic pressures up to 50 GPa. Both materials undergo pressure-induced hexagonal-to-tetragonal structural transformation; however, the calculated phase equilibrium pressures diverge significantly. The Al_3BC_3 undergoes a polymorphic phase transformation at a much higher pressure, i.e., 24 GPa, compared to that for Mg_3BN_3, i.e., ~2 GPa. We proposed a homogeneous orthorhombic in-plane deformation transformation path linking the two end polymorphs. Moreover, the calculated transformation enthalpy barrier is only 0.129 eV/atom for Al_3BC_3 under 24 GPa, which ensures the phase transformation being readily occurred at the predicted pressure. We hope the predicted polymorphism in Al_3BC_3 could be identified in experiment soon.

Acknowledgment

This work was supported by the National Outstanding Young Scientist Foundation for Y.C. Zhou under Grant No. 59925208, Natural Sciences Foundation of China under Grant Nos. 50232040, 50302011 and 90403027, '863' project, and High-tech Bureau of the Chinese Academy of Sciences.

References

[1] R. Riedel, Adv. Mater. 6 (1994) 549–560.
[2] H. Hillebrecht, F.D. Meyer, Angew. Chem. Int. Ed. Engl. 35 (1996) 2499–2500.
[3] C. Jardin, H. Hillebrecht, J. Bauer, J.-F. Halet, J.-Y. Saillard, R. Gautier, J. Solid State Chem. 176 (2003) 609–614.
[4] V.L. Solozhenko, F.D. Meyer, H. Hillebrecht, J. Solid State Chem. 154 (2000) 254–256.
[5] J.Y. Wang, Y.C. Zhou, T. Liao, Z.J. Lin, Appl. Phys. Lett., in press.
[6] H. Hiraguchi, H. Hashizume, O. Fukunaga, A. Takenaka, M. Sakata, J. Appl. Crystallogr. 24 (1991) 286–292.
[7] H. Hiraguchi, H. Hashizume, S. Sakaki, S. Nakano, O. Fukunaga, Acta Crystallogr. B 49 (1993) 478–483.
[8] M.D. Segall, P.L.D. Lindan, M.J. Probert, C.J. Pickard, P.J. Hasnip, S.J. Clark, M.C. Payne, J. Phys.: Condens. Matter 14 (2002) 2717–2744.
[9] D. Vanderbilt, Phys. Rev. B 41 (1990) 7892–7895.
[10] H.J. Monkhorst, J.D. Pack, Phys. Rev. B 16 (1977) 1748–1749.
[11] B.G. Pfrommer, M. Côté, S.G. Louie, M.L. Cohen, J. Comp. Phys. 131 (1997) 233–240.
[12] J.Y. Wang, Y.C. Zhou, Phys. Rev. B 69 (2004) 144108.
[13] J.Y. Wang, Y.C. Zhou, Phys. Rev. B 69 (2004) 214111.
[14] J.Y. Wang, Y.C. Zhou, Z.J. Lin, F.L. Meng, F. Li, Appl. Phys. Lett. 86 (2005) 101902.
[15] J.Y. Wang, Y.C. Zhou, Z.J. Lin, Appl. Phys. Lett. 87 (2005) 051902.
[16] F. Birch, J. Geophys. Res. 83 (1978) 1257–1268.
[17] S. Limpijumnong, W.R.L. Lambrecht, Phys. Rev. Lett. 86 (2001) 91–94.
[18] S. Limpijumnong, S. Jungthawan, Phys. Rev. B 70 (2004) 054104.